

High-temperature fcc phase of Pr: Negative thermal expansion and intermediate valence stateA. Yu. Kuznetsov,^{1,2} V. P. Dmitriev,¹ O. I. Bandilet,¹ and H.-P. Weber^{1,2}¹Group "Structure of Material under Extreme Conditions," Swiss-Norwegian Beam Lines at ESRF, BP220, 38043 Grenoble Cedex, France²Institute of Crystallography, University of Lausanne, CH-1015 Lausanne, Switzerland

(Received 17 March 2003; revised manuscript received 14 May 2003; published 18 August 2003)

A high-temperature angle-dispersive synchrotron radiation diffraction study has revealed the double hexagonal-close-packed-to-face-centered-cubic (dhcp-to-fcc) transformation in the Pr metal occurring martensitically between 575 and 1035 K. The high-temperature fcc phase shows a negative thermal expansion in the range 600–800 K, attributed to the $4f$ -electron delocalization. A phenomenological theory is developed, which explains consistently the observed effect in terms of the mean valence variation of the metal as a function of temperature; it also predicts the existence of an isostructural phase transition and of a critical end point of a gas-liquid type in compressed Pr. The analysis of published data on P - T variation of conductivity of Pr supports this prediction.

DOI: 10.1103/PhysRevB.68.064109

PACS number(s): 61.66.Bi, 64.70.-p, 65.40.De, 71.20.Eh

I. INTRODUCTION

Despite the successful extension of the phase diagrams of lanthanide metals into the high-pressure region, information about low-pressure transformations and high-temperature phases are in some cases still insufficient and unreliable. Surprising features of low-pressure transitions between four-layered double hexagonal-close-packed (dhcp) and three-layered face-centered-cubic (fcc) structures in La, Pr, and Nd have been reported (see review paper¹). In these three metals, the dhcp structure is known to be stable at ambient pressure and temperature. The stability domain of the fcc phase, however, is mapped with great uncertainty; conflicting data have been published about the low-pressure region ($P < 2$ GPa) at elevated temperatures ($T > 500$ K). At ambient pressure the dhcp-to-fcc transformation has been observed only in La ($T_{\alpha-\beta} = 580$ K) (Refs. 2,3) while data reported on Pr and Nd are contradictory. On one hand, one can find earlier publications reported on the dhcp-bcc (but not the dhcp-fcc) transformation at $T = 1070$ K in Pr and $T = 1140$ K in Nd.³ On the other hand, in these metals a metastable fcc phase was retained at room temperature by quenching (splat cooling) in an arc furnace.⁴ In later studies, the dhcp-to-fcc transformation was observed in the course of combined pressure-temperature variations.^{5,6} However, the convergence of the hysteretic region between the dhcp and fcc phases, in La, Pr, and Nd correlated with the gradual disappearance of the corresponding jumplike anomaly in electrical conductivity and this is how the P - T phase diagram of these metals in the low-pressure region was established.^{5,6} These effects are characteristic for the cross-over from a first-order to a *second-order* transformation regime, but such tricritical behavior is not permitted for a *reconstructive* dhcp-fcc transformation. For this reason, the dhcp-fcc transition boundary has not yet been charted in the low-pressure region, and there is no certitude either as to the existence or the absence of the dhcp-fcc transformation at ambient pressure (Fig. 1).

In the present work, we confirm experimentally the existence, at ambient pressure, of the dhcp-to-fcc transformation

in Pr and present some interesting properties of Pr metal in the high-temperature fcc phase.

II. EXPERIMENTAL METHODS

In situ high-temperature data were obtained at the Swiss-Norwegian beam lines of the European Synchrotron Radiation Facility (ESRF, Grenoble, France). X-ray-diffraction patterns were collected in angle-dispersive geometry on an image plate detector (MAR345) with unfocused monochromatic beam at wavelength $\lambda = 0.700(0)$ Å. The sample-to-detector distance and the image plate inclination angles were precisely calibrated using a silicon standard. Two-dimensional diffraction images were analyzed using the ESRF Fit2D software, yielding one-dimensional intensity vs diffraction angle 2θ patterns.⁷ Two different heating setups were used to speed up the expected phase transformations. One can expect such an increase in the transformation rate in

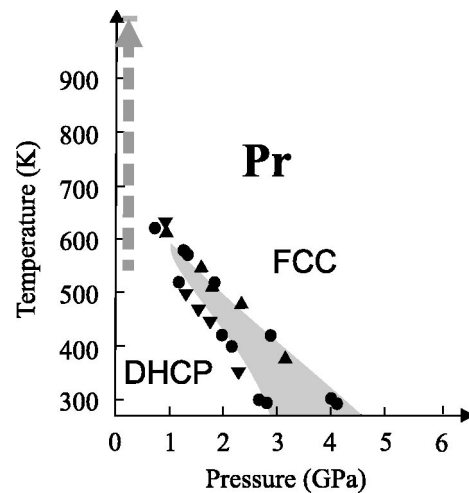


FIG. 1. Partial P - T phase diagram of Pr metal. Shaded is "region of indifference"¹. Experimental points taken from Ref. 5 correspond to discontinuities in the electrical conductivity. Dashed arrow shows the dhcp/fcc two-phase region as observed in present work.

nonequilibrium thermal conditions in the presence of temperature gradients; such gradients are known to remove eventual crystal imperfections that act as internal obstacles in course of the dhcp-fcc phase transition. For this reason we employed two different devices: (a) a Lincam DT-1500 temperature cell (high-temperature limit is 1600 K), the features of which are a small sample volume heated by a flat heater and a permanent flow of high purity inert gas across the cell, (b) a tubular furnace where the heating coil surrounded the sample (limited to 1100 K).⁸ The Linkam furnace yielded stationary thermal conditions with high gradients across the sample while the tubular furnace provided equilibrium thermal conditions but with a reduced upper temperature limit.⁸ It should be pointed out that, in contrast with an equilibrium heating setup, a nonequilibrium one does not allow us to control experimental conditions except an average temperature. Therefore, to characterize quantitatively the thermal expansion of Pr, only data collected under equilibrium heating conditions were used.

The samples used consisted of filings of polycrystalline Pr metal (99.9% purity, Goodfellow). All manipulations were performed in an inert atmosphere (Ar or He of high purity) in order to prevent oxidation of the samples. In case of the tubular furnace the filings were loaded in capillaries, furnished with ultrahigh-purity He gas, and pumped out to high (10^{-5} mbar) vacuum and sealed. With the Lincam DT-1500 cell, the filings were loaded directly in a glove bag and during all experiments the samples were kept under the permanent flow of a high-purity inert gas (Ar or He).

III. RESULTS AND DISCUSSIONS

A. dhcp to fcc transformation

Figure 2 shows selected angle-dispersive x-ray diffraction patterns of Pr metal in the temperature range including the dhcp-to-fcc transformation at ambient pressure. All peaks could be indexed with the fcc and dhcp structures. The transformation is obviously sluggish and develops throughout the two-phase region. The first indication of the fcc phase appears in Pr at about 575 K, under equilibrium as well nonequilibrium conditions ($a_{fcc}^{eq} = 5.134 \text{ \AA}$). The intensity of the fcc peaks increases with rising temperature, while the intensity of the dhcp peaks decreases continuously (Fig. 2). The Debye-Scherrer diffraction patterns show a progressive recrystallization of the sample, even at low temperatures: the initially homogeneous diffraction rings, belonging to the dhcp structure, transform into spotty ones. The fcc diffraction patterns appear first as perfectly isotropic broadened rings [Fig. 3(a)], indicating initially random orientation of numerous nucleation centers. The fcc diffraction rings remain homogeneous over a considerable temperature range but decrease in width with increasing temperature, the effect corresponding to an increase in crystallite size. Further evolution of the fcc rings is similar to that of dhcp; they also turn spotty [Fig. 3(b)], the result of the preferred growth of selected nuclei. In the equilibrium thermal conditions, a considerable amount of the dhcp phase remains untransformed up to the fcc-bcc transition point ($T = 1070 \text{ K}$) while under nonequilibrium conditions the Pr sample becomes fcc single

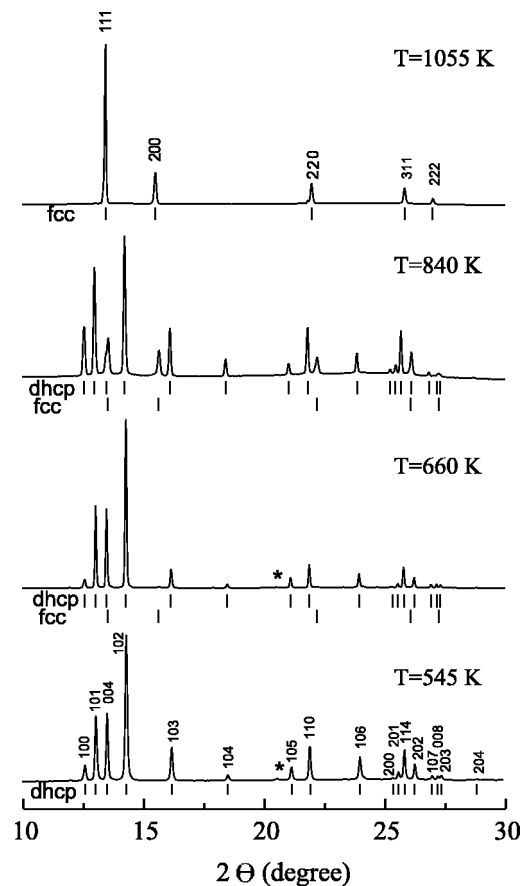


FIG. 2. Selected high-temperature synchrotron radiation x-ray powder diffraction patterns of Pr metal in different phases at ambient pressure (nonequilibrium conditions). Asterisks denote weak PrH_2 peaks. The tick marks indicate the positions of calculated Bragg reflections.

phased at about $T = 1035 \text{ K}$ [Figs. 2 and 3(b)]. Thus there can be no doubt that the dhcp-to-fcc isobaric transformation in Pr does occur. It is worth noting that the kinetics of this isobaric transformation is very similar to the pressure-induced martensitic dhcp-fcc transformation in Pr.¹

B. Thermal expansion

The properties of the cubic phase of Pr are very intriguing. Figure 4 shows the temperature dependence of the

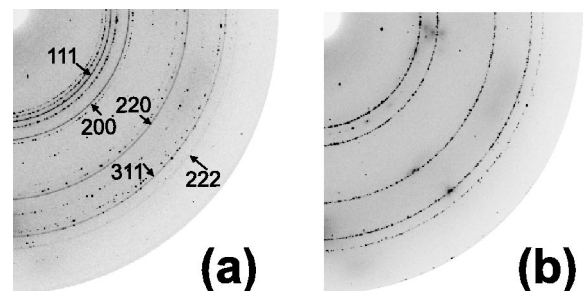


FIG. 3. Debye-Scherrer diffraction rings of Pr as recorded on an image plate. (a) $T = 840 \text{ K}$; fcc diffraction rings are indexed. (b) $T = 1055 \text{ K}$.

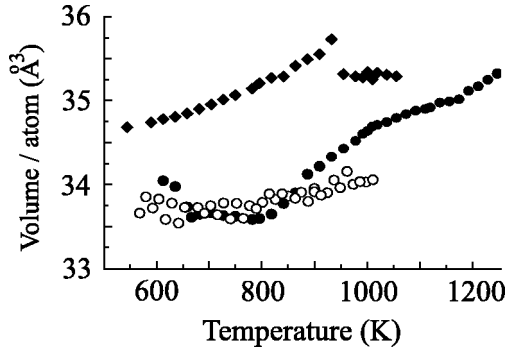


FIG. 4. Temperature dependence of the atomic volume of Pr metal. Circles—fcc phase in equilibrium (open) and nonequilibrium (solid) conditions; diamonds—dhcp phase in nonequilibrium conditions.

atomic volume of the dhcp and fcc Pr. Remarkable is the behavior of the latter in the range between 550 K and 800 K. One notes that the cubic structure has initially a negative thermal expansion coefficient. It then changes its sign but still keeps an anomalously low (almost zero) value over a wide temperature region and only starts exhibiting a normal temperature expansion from about 800 K upward. In contrast, the dhcp structure shows in the same temperature range a smooth increase of the thermal expansion coefficient α_V fitted by the curve

$$\alpha_V^{dhcp} = (1.45 \times 10^{-4}) - (9.141 \times 10^{-7})T + [(1.796 \times 10^{-9})T^2 - (9.32 \times 10^{-13})T^3].$$

However, the remaining dhcp phase also exhibits a small but visible (about 1.2%) negative volume jump at $T \approx 950$ K, and then the volume variation of the collapsed dhcp phase is similar to that for the fcc phase but at a lower temperature ($650 \text{ K} < T < 800 \text{ K}$). This behavior can be seen even more spectacularly in the variation of the interlayer spacing $d_{[111]c}$, which is compared, in Fig. 5, with its hexagonal analog $d_{[004]h}$ (both are d spacings between hexagonal-close-packed atomic planes). Again, one can see a monotonic increase in the dhcp interlayer distance interrupted, at 950 K, by a downward jump. In contrast with the dhcp structure, the fcc structure first shows a negative thermal expansion and then a stabilization of the lattice parameter. Except for some details, the lattice parameters in equilibrium heating conditions show a similar temperature behavior. One can see that the linear thermal expansion coefficient along the c axis, α_L^c , of dhcp structure increases smoothly from $1.273 \times 10^{-5} \text{ K}^{-1}$ to $2.023 \times 10^{-5} \text{ K}^{-1}$ in the 300–900 K temperature range, while the fcc structure shows a typical Invar-type behavior [Figs. 5(b,c)]. The evident temperature scaling between nonequilibrium and equilibrium datasets can be attributed to the particularity of the transformation process, namely, a slower kinetics under the equilibrium heating conditions.

In search of an explication for the observed phenomenon, one can suggest several mechanisms for the lattice contraction or lattice spacing temperature stabilization. The first one, the Invar effect proper, is due to a coupling between the

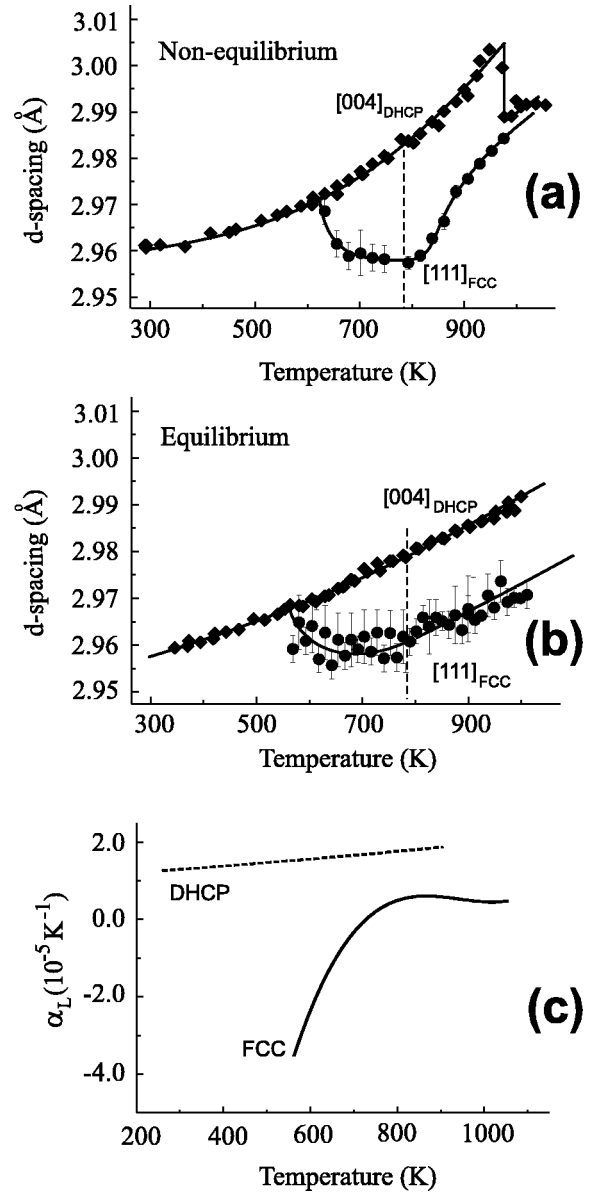


FIG. 5. Linear thermal expansion of Pr metal: (a) nonequilibrium conditions; (b) isotropic heating. Diamonds correspond to the dhcp phase, and circles to the fcc phase. (c) Smoothed linear expansion coefficients α_L^c (dashed line) and α_L^{fcc} (solid line).

spontaneous strain components and the magnetization vector components arising at the transition into a ferromagnetically or antiferromagnetically ordered phase. The spontaneous magnetostrictive effect compresses the crystal lattice, and thus can compensate its thermal expansion.⁹ However, this mechanism is not applicable here since polycrystalline dhcp Pr orders antiferromagnetically only below 25 K (Ref. 10) and fcc Pr, stabilized at ambient pressure, orders ferromagnetically below 8.7 K.⁴

It is known that transverse vibrational modes can lead to a negative thermal expansion (see, for example, review paper¹¹); however, this mechanism is operational only in complex materials. This is not the case for elemental Pr.

The mechanism most consistent with our experimental observation relates to the valence transition reported for sev-

eral rare-earth metals. These metals are known to exhibit a valence variation with pressure and temperature¹² accompanied by a corresponding *lattice contraction*. The best known example is the isostructural $\gamma(\text{fcc})-\alpha(\text{fcc}')$ phase transition in Ce metal, which is characterized by a considerable ($\sim 20\%$) atomic volume collapse (see review Ref. 13). Two microscopic models were proposed to explain this effect; they are both based on the concept of the *intermediate valence*.¹⁴ The first one considers the intermediate valence state as a temporal one, that is, in the intermediate state the ions *fluctuate* between the two pure ionic configurations.¹⁴ The other model considers the system as an *alloy* of constituents of different integral valence (+3 and +4 in the Ce case) and treats the intermediate state in the virtual-crystal approximation.^{15,16} A discussion on the details and advantages of each approach is beyond the scope of the present paper. However, since they both allow the existence of intermediate values for valence, one can use this latter as a smoothly variable parameter for a phenomenological model irrespective of the microscopic nature of such a variation. The valence variation between the low- and high-valence limits evidently should yield variation of the lattice constants in the sense that they attain values corresponding to $n + \Delta$ ($0 \leq \Delta \leq 1$), intermediate to those expected for pure n - and $(n + 1)$ -valence metal.

C. Phenomenological model

In this section, we consider the phenomenological model of the valence variation effect in Pr and show a consistency between phenomena observed in Ce and Pr metals. Experimental evidences for valence variation, i.e., the existence of intermediate valence states, were reported for at least three members of the rare-earth metal family: Ce,¹⁷ Eu,¹⁸ and Yb (Ref. 19) (see also Ref. 12 and references therein). In Ce a discontinuous variation of the valence was found to cause the observed isostructural $\gamma(\text{fcc})-\alpha(\text{fcc}')$ transformation through the corresponding atomic volume collapse. In contrast, in Eu, the valence varied continuously over a wide pressure range including the bcc-hcp phase boundary, and no remarkable anomalies in the lattice parameter behavior were observed. Both types of variations, continuous and discontinuous, can be treated within the framework of an unified phenomenological model of an isostructural phase transition. Such a Landau-type theoretical approach is known to deal with a single-component order parameter spanning the totally symmetrical (identity) irreducible representation of the parent phase-space group. A scalar (isotropic) physical quantity, such as volume or valence deviation, perfectly fits this role.

Since our inferred existence of an intermediate valence state in elemental Pr is, to our knowledge, first of its kind and the variety of experimental datasets is restricted to thermal expansion, we will limit also the theoretical model to the minimal form, choosing the minimal set of the corresponding phenomenological parameters, and consider their variation in the vicinity of the critical point. This approximation will receive *a posteriori* experimental support.

The nonequilibrium energy (Landau potential) associated with the simplest model of an isostructural phase transition has the form

$$F(\eta) = a_1 \eta + a_2 \eta^2 + a_3 \eta^3 + \eta^4, \quad (1)$$

where η is the totally symmetrical (nonsymmetry breaking) order parameter, and a_i are phenomenological parameters. The change of variables $\eta = \Delta - a_3/4$ and following elimination of the equilibrium part of the energy transforms Eq. (1) into the normal form:

$$F(\Delta) = \tilde{a}_1 \Delta + \tilde{a}_2 \Delta^2 + \Delta^4, \quad (2)$$

where $\tilde{a}_1 = a_1 - a_2 a_3/2 + a_3^3/8$, and $\tilde{a}_2 = a_2 - 3a_3^2/8$. Minimization of the potential $F(\Delta)$ with respect to the order parameter Δ yields an equation of state as follows:

$$\frac{\partial F}{\partial \Delta} = \tilde{a}_1 + 2\tilde{a}_2 \Delta + 4\Delta^3 = 0. \quad (3)$$

It is not necessary to investigate here the above model in detail since the form of the Landau potential (2) coincides with one of the *elementary catastrophes* (namely, the cusp catastrophe), and was studied comprehensively in the framework of the mathematical *catastrophe theory*.²⁰ The equilibrium values of the order parameter Δ , which we will choose as the metal valence deviation, are the solutions of the equation of state (3); and because this is a cubic equation, it has either one or three real roots, and only those have a physical meaning. The number of roots is determined by the determinant $D = 8\tilde{a}_2^3 + 27\tilde{a}_1^2$. If $D \leq 0$ there are three *real* roots:

$$\Delta_{1,2,3} = -2\rho \cos \frac{\varphi}{3}, \quad \Delta_{2,3} = 2\rho \cos \frac{\pi \pm \varphi}{3};$$

$$\rho = \text{sgn } \tilde{a}_1 \sqrt{|\tilde{a}_2/6|}, \quad \cos \varphi = \tilde{a}_1/8\rho^3, \quad (4)$$

two ($\Delta_{2,3}$) corresponding to minima of the Landau potential and one (Δ_1) corresponding to a maximum; otherwise there is only one (Δ_1). Figures 6(a) and 6(b) illustrate this by a three-dimensional (3D) diagram of the equilibrium surface (3) and its projection on the \tilde{a}_1 - \tilde{a}_2 plane. It is easy to predict the valence magnitude behavior for the different paths, i.e., on the different plane sections of the equilibrium surface. One can see that smooth variations in \tilde{a}_1 and \tilde{a}_2 almost always produce smooth variation in Δ . The only exceptions occur when the system crosses the energy equality (isostructural first-order phase transition) line $F(\Delta_2) = F(\Delta_3)$, i.e., $\tilde{a}_1 = 0$. In this point it jumps to the other sheet corresponding to the other energy minimum ($\Delta_2 \leftrightarrow \Delta_3$). This brings about a sudden change in Δ . The projection of the folds of the equilibrium surface onto the \tilde{a}_1 - \tilde{a}_2 plane ($D = 0$, $\tilde{a}_2 = 3\tilde{a}_1^{2/3}/2$) are the stability limit (spinodal) lines for the low- and high-valence states [Fig. 6(b)]. The variation regime in Δ can be changed smoothly from discontinuous to continuous by varying the \tilde{a}_2 parameter from negative to positive sign. The change of regime occurs at $\tilde{a}_2 = 0$, i.e., at the critical point (CP) of the liquid-gas type [Figs. 6(a) and 6(b)].

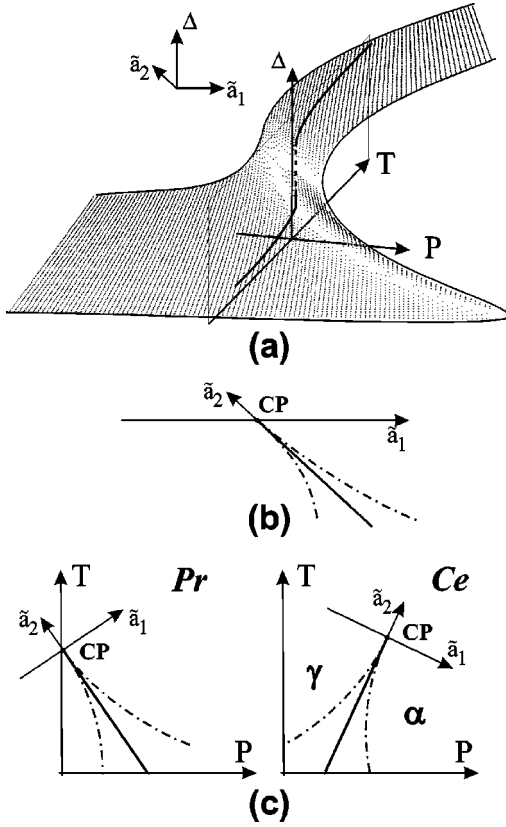


FIG. 6. (a) Equilibrium surface corresponding to Eq. (3). (b) Projection onto the \tilde{a}_1 - \tilde{a}_2 plane. Dashed-dotted lines are stability limit lines, solid line—the first-order isostructural phase transition line. CP is the critical point. (c) Schematic position of the isostructural phase transition lines on the P - T phase diagrams of Pr and Ce.

In order to map the phase boundaries experimentally measured in the P - T coordinate system onto the 2D space of the phenomenological parameters \tilde{a}_1 - \tilde{a}_2 , a linear transformation is called for

$$\begin{aligned}\tilde{a}_1(T, P) &= \alpha_1(T - T_0) + \beta_1(P - P_0), \\ \tilde{a}_2(T, P) &= \alpha_2(T - T_0) + \beta_2(P - P_0).\end{aligned}\quad (5)$$

This establishes the $(P, T) \Leftrightarrow (\tilde{a}_1, \tilde{a}_2)$ correspondence, using a minimal number of fitting parameters α_i , β_i , T_0 , and P_0 . Both coordinate systems are shown in Fig. 6(a) along with an example of the isobaric variation of the order parameter Δ .

D. Valence variation

Our experimental data on equilibrium thermal expansion [Fig. 5(b)] can be recalculated into the valence temperature variation by using the alloy model. For this purpose we can consider, without loss of generality, the elemental Pr crystal as a solid solution of x fraction of tetravalent and $(1-x)$ fraction of trivalent metal. An average metallic radius of Pr atom, which determines interatomic distances and lattice parameters of such a “disordered alloy,” is equal to $R = xR^{4+} + (1-x)R^{3+}$, where $R^{3+} = 1.83 \text{ \AA}$ corresponds to the trivalent $4f^3 5d^0 6s^2$ electron configuration and $R^{4+} = 1.658 \text{ \AA}$ corresponds to the tetravalent $4f^2 5d^1 6s^2$ one. The latter nu-

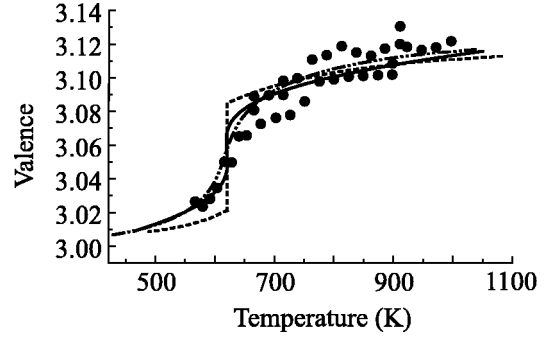


FIG. 7. Praseodymium valence variation in the fcc phase, data from three different experimental runs in isotropic heating conditions are used. Lines show the theoretically predicted valence behavior for the path far from the critical point, $\tilde{a}_2 < 0$ (dashed), at the critical point, $\tilde{a}_2 = 0$ (solid), and beyond the critical point, $\tilde{a}_2 > 0$ (dashed dotted).

merical estimation is taken from Ref. 21, and R is obtained from the experimental values for d spacings. Then, in order to get the *contractive* part of the atom size variation, the difference $\Delta d = d_{[111]}^{fcc} - d_{[004]}^{dhcp}$ [Fig. 5(b)] can be used. One can find the values for intermediate valence of Pr taking into account that $x \equiv \Delta$ and using an equation identical to that for atomic radius R , $v = 4\Delta + 3(1 - \Delta)$.

Figure 7 shows the temperature variation of the valence in the fcc phase of Pr metal obtained as just described. Three curves represent sections of the equilibrium surface (3) [Fig. 6(a) and Eqs. (4)] in the vicinity of the critical point. One can see that the experimental point distribution corresponds to the thermodynamic path passing very close to the critical point, in the domain of smooth variation of the order parameter ($\tilde{a}_2 \geq 0$).

The sign and character of the volume and of the valence variations allows us to suggest the position of the line of the isostructural phase transition in the P - T phase diagram of Pr, which is compared with that for Ce in Fig. 6(c). One can see that, different from Ce, the line of the isostructural transformation in Pr should have a negative slope.

As a final remark, we should point out the difference in valence behavior of fcc and dhcp Pr. In the latter, the valence varies; and, therefore, the volume collapses at higher temperatures. Obviously, a phenomenological consideration is not capable to explain such a difference. However, this is a good challenge for a first-principles calculation as successfully carried out previously in order to describe electronically driven effects in lanthanide metals. On the phenomenological level, one can argue only about the different site symmetry of metal atoms in fcc (s.s. $m\bar{3}m$) and dhcp (s.s. $\bar{3}m$ and $\bar{6}m2$) structures as a possible reason for the electron transition retardation.

E. Hypothesis

The question arises as to the occurrence, in earlier publications, of the phenomenon described in the present paper? Let us analyze the data on Pr conductivity anomalies ob-

tained by the authors of Ref. 5 and interpreted by them as induced by the dhcp-fcc transformation. It has already been mentioned that the convergence of the hysteretic region (Fig. 1) and the vanishing of the conductivity anomaly are not compatible with the reconstructive character of the dhcp-to-fcc transformation.²² Thus, our diffraction data reveal a sluggish kinetics of the dhcp-to-fcc transformation in Pr and no increase in the rate of transformation at high temperatures and, therefore, throws doubt on the origin of such *jumplike* anomaly. However, our proposed model clarifies the phenomenon.

The sluggish character of the dhcp-fcc transformation, due to the gradual nucleation of the new phase, does not allow one to predict a discontinuous character of the sample conductivity behavior, even when the difference in the individual phase conductivities is considerable. In fact, the deviation of the conductivity should correlate with the amount of the new phase, the variation of which was found experimentally to be smooth. One should remember that there is also no thermodynamic justification for the crossover from discontinuous to continuous character of the transformation.

The contradiction can be resolved if one assumes an electronic origin for the conductivity anomaly, i.e., a $4f$ electron *delocalization* with a corresponding valence variation. In addition, the *negative* sign of ΔR observed in Pr (Ref. 5) coincides with that observed at the isostructural γ - α transition in Ce and perfectly correlates with electron delocalization mechanism, while the succeeding α - α' polymorphic trans-

formation induces the *increase* in resistivity.²³ Thus, our phenomenological model, based on the valence variation mechanism (Sec. III C, Fig. 6), allows one to understand the nature of the effect and suggests that the line of the isostructural phase transition in Pr was already mapped in Ref. 5.

IV. CONCLUSION

Our x-ray diffraction study at high temperatures showed that Pr metal undergoes a phase transition from dhcp to fcc in the temperature range 575–1035 K. The evolution of the corresponding diffraction patterns was found to be very similar to the pressure-induced dhcp-fcc transformation observed at room temperature, indicating a martensitic character of this transformation. An Invar-like behavior of the lattice parameters was found for the high-temperature cubic phase and attributed to an interaction between normal thermal expansion and contraction induced by valence variation, the latter being observed for the first time in metallic Pr.

ACKNOWLEDGMENTS

Experimental assistance from the staff of the Swiss-Norwegian Beam Lines at the ESRF is gratefully acknowledged. This work was supported in part by Grants No. 21-45703.95 and 21-68141.02 from the Swiss National Science Foundation.

-
- ¹T. Kruger, B. Merkau, W.A. Grosshans, and W.B. Holzapfel, High Press. Res. **2**, 193 (1990).
- ²*Handbook on the Physics and Chemistry of Rare Earths*, edited by K. A. Gschneidner, Jr., and L. Eyring (North-Holland, Amsterdam, 1986), Vols. 1–32.
- ³K. A. Gschneidner, Jr., and F. W. Calderwood, in *Handbook on the Physics and Chemistry of Rare Earths* (Ref. 2), Vol. 8, p. 1.
- ⁴E. Bucher, C.W. Chu, J.P. Maita, K. Andres, A.S. Cooper, E. Buehler, and K. Nassau, Phys. Rev. Lett. **22**, 1260 (1969).
- ⁵N.A. Nikolaev, L.G. Khvostantsev, V.E. Zinov'ev, and A.A. Starostin, Sov. Phys. JETP **64**, 589 (1986).
- ⁶N.A. Nikolaev and L.G. Khvostantsev, Sov. Phys. JETP **65**, 205 (1987).
- ⁷A.P. Hammersley, S.O. Svensson, M. Hanfland, A.N. Fitch, and D. Hausermann, High Press. Res. **14**, 235 (1996).
- ⁸M. Estermann, H. Reifler, W. Seurer, F. Filser, P. Kocher, and L.J. Gauckler, J. Appl. Crystallogr. **32**, 833 (1999).
- ⁹E. F. Wasserman, in *Ferromagnetic Materials*, edited by K. H. J. Buschow and P. Wolhlfarth (North-Holland, Amsterdam, 1990), Vol. 5, p. 237.
- ¹⁰J.W. Cable, R.M. Moon, W.C. Koehler, and E.O. Wollan, Phys. Rev. Lett. **12**, 553 (1964).
- ¹¹J.O.S. Evans, J. Chem. Soc. Dalton Trans. **1999**, 3317.
- ¹²J. Röhler, in *Handbook on the Physics and Chemistry of Rare Earths* (Ref. 2), Vol. 10, p. 453.
- ¹³D. C. Koskenmaki and K. A. Gschneider, Jr., in *Handbook on the Physics and Chemistry of Rare Earths* (Ref. 2), Vol. 1, p. 337.
- ¹⁴M.B. Maple and D. Wohlleben, Phys. Rev. Lett. **27**, 511 (1971).
- ¹⁵I.L. Aptekar' and E.G. Ponyatovsky, Phys. Met. Metallogr. **25**, 10 (1968).
- ¹⁶A. Rosengren and B. Johansen, Phys. Rev. B **13**, 1468 (1976).
- ¹⁷J. Röhler, D. Wohlleben, J.P. Kappler, and G. Krill, Phys. Lett. **103A**, 220 (1984).
- ¹⁸J. Röhler, Physica B & C **144**, 27 (1986).
- ¹⁹K. Syassen, G. Wortmann, J. Feldhaus, K.H. Frank, and G. Kaindl, Phys. Rev. B **26**, 4745 (1982).
- ²⁰See, e. g., the fundamental book by T. Poston and I. N. Stewart, *Catastrophe Theory and its Applications* (Pitman, London, 1978); and also a review paper full of the physical meaning: E.T. Kut'in, V.L. Lorman, and S.V. Pavlov, Sov. Phys. Usp. **34**, 497 (1991).
- ²¹S. H. Liu, in *Handbook on the Physics and Chemistry of Rare Earths* (Ref. 2), Vol. 1, p. 233.
- ²²P. Tolédano and V. Dmitriev, *Reconstructive Phase Transitions in Crystals and Quasicrystals* (World Scientific, Singapore, 1996).
- ²³L.G. Khvostantsev and N.A. Nikolaev, Phys. Status Solidi B **114**, K135 (1982).